# Self-Aggregation of the SDS Surfactant at a Solid−Liquid Interface

**Hector Domínguez***

*Instituto de Investigaciones en Materiales, UNAM. Universidad Nacional Autónoma de México, México, D.F. 04510*

*Received: November 22, 2006; In Final Form: February 19, 2007*

Molecular dynamics simulations of sodium dodecyl sulfate (SDS) molecules on a graphite surface are presented. The simulations were conducted at low and high surface coverage to study aggregation at the water/graphite interface. Results showed that at low surface coverage, the SDS molecules form hemicylindrical aggregates, in agreement with AFM experiments, whereas at high surface coverage, the surfactants form full cylinders. The latter aggregates have not been reported in systems of SDS on hydrophobic substrates, such as graphite. The unexpected results are explained in terms of a water layer adsorbed at the solid surface which was the responsible for the formation of these aggregates. Moreover, the SDS tails in the full cylindrical configuration became straighter than those of the hemicylindrical aggregate. Hydrogen bond formation between water and surfactant head groups was also studied, and it was found that they did not depend on the surfactant concentration.

## 1. Introduction

Surfactant adsorption studies at interfaces have been investigated not only for their scientific interest but also for their applicability in industrial processes, such as detergency, lubrication, and colloid stabilization. Although several experiments have been conducted to study the behavior of surfactants at liquid/air and liquid/liquid interfaces,[1−8] the self-assembly of surfactants in the presence of a solid surface has been less understood. Therefore, for the last several years, the self-assembly of amphiphilic molecules on surfaces has been widely investigated to study their aggregation at solid plates, since the knowledge of these systems can help us to better understand areas such as absorption or electrochemistry and electrode surfaces.[9]

It is well-known that the self-aggregation of surfactant molecules into spheres, cylinders, and bilayers in bulk solutions, how aggregation is modified by the presence of solid surfaces, is not very clear. Several experiments suggest that most of the aggregates observed in bulk solutions can also appear at the solid/liquid interface.[9−13] However, the nature, the structure and the shape of these aggregates present different features due to the extra solid−surfactant interaction. Therefore, several studies on different hydrophobic and hydrophilic surfaces, such as graphite, silica, mica, etc., have been conducted using different experimental techniques.[14−18] A valuable technique to study the self-assembly of surfactants (ionic and nonionic) adsorbed from aqueous solution on different solid surfaces is atomic force microscopy (AFM).[9,13,19−22] From AFM experiments, people have observed how surfactant concentration affects aggregation. For instance, experiments of sodium dodecyl sulfate (SDS) on graphite showed hemicylindrical aggregates at concentrations above one-fourth of the critical micelle concentration (cmc), whereas below this concentration, any structure was found.[23] Different experimenters have reported aggregation at lower SDS concentration in the presence of NaCl by using AFM;[23] other authors have reported the effects of the surfactant chain length[12] and the surfactant headgroup[20] in the self-assembly of surfactant molecules at the solid/liquid interface.

From experimental results, there is a general agreement that surfactants on hydrophobic surfaces (e.g., graphite) self-organize in hemicylinders, since hydrophobic substrates interact primarily with the tail groups through the van der Waals forces. In this case, the alkane chains are adsorbed on the graphite plates (due to epitaxy),[13,24] forming half cylindrical aggregates on the surfaces. However, hydrophilic substrates interact primarily with the surfactant head groups, giving rise to different aggregates on the surfaces, such as full cylinders or spheres. Therefore, surfactant adsorption seems to be affected by the characteristics of the surface.

In particular, from AFM, it has been observed that the SDS surfactant forms hemicylinders on graphite[23] and also on hydrophobic solid gold surfaces.[9] On the other hand, people have seen that the $C_{14}$TAB surfactant aggregates in half-cylinders on hydrophobic substrates, full cylinders on mica, and spheres on amorphous silica.[19] However, the formation of different aggregates of the same surfactant on the same hydrophobic (or hydrophilic) substrate has not been observed or reported.

Due to the increase in computer power over the last years, computer simulations have become an important tool for the study of such complex interfacial systems. Computer techniques allow us to extract more information about dynamical, thermodynamical, and structural properties of interfacial problems from a molecular level that sometimes are not easy to obtain from real experiments. Therefore, simulations from fully atomistic[25−27] to coarse-grain models[28−31] have been reported in the literature to investigate those systems. For instance, Srinivas et at. investigated the formation of structures depending on the alkyl chain length.[28] They observed that surfactants with short chains form monolayers, whereas surfactants with longer tails form hemicylinders on a graphite surface. In the present work, we studied the adsorption of SDS molecules on a graphite surface, and we investigated the aggregation of the surfactants at two

* To whom correspondence should be addressed. E-mail: hectordc@servidor.unam.mx.

10.1021/jp067768b CCC: $37.00 
Published on Web 03/30/2007

different surface coverages. The system was chosen because experimental data[9,23] were available to allow us to make comparisons, in some cases, with the present results.

## 2. Computational Method and Model

Simulations of the anionic (SDS) molecule with a model of a hydrocarbon chain of 12 united carbon atoms attached to a head group, $SO_4$, were performed. The head group atoms were explicitly modeled, and the simulation parameters for the SDS were the same as those used in previous works.[32,33] For the liquid phase, we used the SPC water model, and the solid surface was constructed of two layers of graphite plates using an atomistic model.

From experimental and computational analysis, we know that surfactants aggregate at the solid surface due to the new surfactant−solid interaction. Therefore, the initial configuration was prepared from a monolayer of 36 surfactant molecules in all-trans configuration, with the SDS head groups initially pointed to the solid surface, placed close to the graphite square surface of dimensions $X$ and $Y = 40.249$ Å. Then 2416 water molecules were added to the system, and 36 sodium cations ($Na^+$) were also included. The usual periodic boundary conditions were imposed in the simulations; however, the $z$-dimension of the box was set to 150 Å. This length was long enough to prevent the formation of a second water/solid interface due to the periodicity of the system. Instead, a liquid/vapor interface was present at one end of the box ($z > 0$, i.e., a bulk water region was formed), whereas at the other end of the box ($z < 0$) beyond the solid graphite, there was an empty space.

In order to study the effects of concentration in the self-organization of the surfactants at the solid/liquid interface, another simulation was conducted. The new system was prepared in the same way as mentioned above; however, we used 81 SDS molecules in this case.

All simulations were carried out in the NVT ensemble using the DL-POLY package[34] with a time step of 0.002 ps. We performed simulations at a temperature of 300 K using the Hoover−Nose thermostat with a relaxation time of 0.2 ps.[35] The long-range electrostatic interactions were handled by the particle mesh Ewald method with a precision of $10^{-4}$, and the van der Waals interactions were cut off at 10 Å. Finally, long simulations were conducted up to 17 ns, during which the last 4 ns were used for data acquisition.

## 3. Results

In this section, we present the calculations performed on the SDS surfactant for two different concentrations. Studies of the behavior of the SDS molecules and how they self-organize at the liquid/solid interface are discussed.

**3.1. Surfactant Structure at the Interface.** The system with 36 SDS molecules at the interface was constructed to have a surface coverage of 45 Å$^2$/molecule, which is the area per headgroup at the critical micelle concentration at the water/vapor interface.[36] Therefore, at this concentration, we expected to observe aggregation, as some experiments indicated.[23]

At this surface coverage, we observed that the SDS headgroups next to the surface were rapidly repelled from the graphite surface. Then the affinity between the graphite atoms and the carbons in the tails made these two groups "prefer" to be closer to each other than the SDS headgroups with the graphite. In Figure 1, snapshots at different simulation times until the SDS molecules self-organize in a hemicylindrical conformation are shown. From Figure 1c to Figure 1d, it is observed that the structure of the aggregate did not change considerably, suggesting a stable configuration. Due to the number of surfactant molecules and the area of the surface used in the simulation, only one aggregate was formed. Nevertheless, interesting features about the structure can be depicted, as we will show.

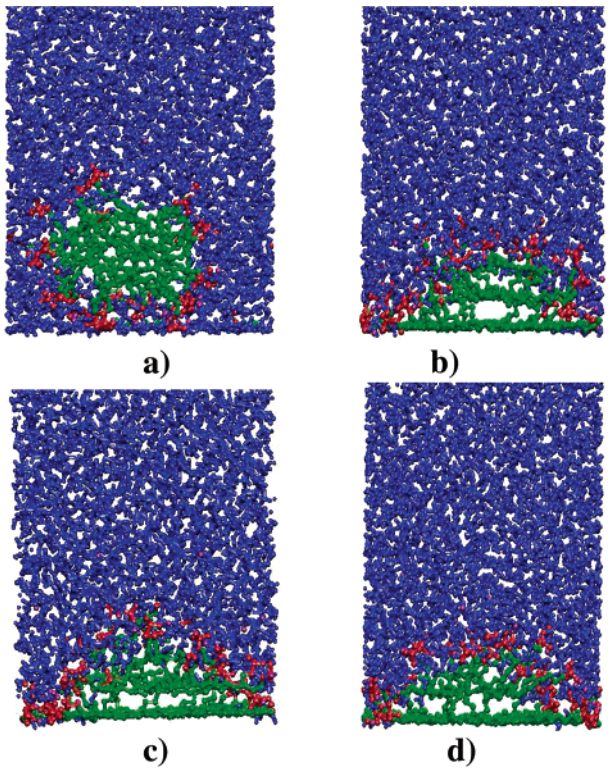


**Figure 1.** Snapshots of the SDS surfactant on a graphite surface at low SDS surface coverage for different simulation times: (a) 800 ps, (b) 9.5 ns, (c) 11.5 ns, and (d) 17.0 ns. Water is shown in blue; SDS headgroups, in red; SDS tails, in green; and the $Na^+$ counterions, in purple. The graphite plate is located at the bottom side of the molecules.

The SDS structure on the graphite surface was analyzed in terms of the density profiles of the molecules. These profiles can give us information of how the molecules array along the interface. Therefore, density profiles were calculated in the $z$-direction, i.e., normal to the liquid/solid interface. In Figure 2, the $z$-dependent density profiles for the water, the headgroups, and the hydrocarbon tails are shown. The interesting feature depicted in those profiles is that the SDS tails were absorbed at the graphite surface as two well-defined layers were formed.

The array of the hydrocarbon chains can also be characterized by the probability of gauche defects, since this quantity can give us more insights about the conformation of the tails; i.e., the gauche probability can give us, somehow, information on the deviation of the tails from the all-trans conformation. The gauche defects were determined by analyzing torsion angles; therefore, if a torsional angle deviates more than ±60° from the all-trans configurations (180°), it is defined as a gauche defect.

In Figure 3, the probability of gauche defects for each carbon in the tail is shown. It was observed that the first dihedral ($S-O-C_1-C_2$) of the SDS tails is almost trans. The second and even the third dihedral present a high gauche defect probability, whereas the probability for the rest of the carbons oscillates, and it decreases at the end of the tails, suggesting that the chains were not completely ordered.

The total length of the tails was measured by the distance from the first to the last carbon in the tails, and we found an average length of $l = 9.6$ Å. Since the total length of the tails

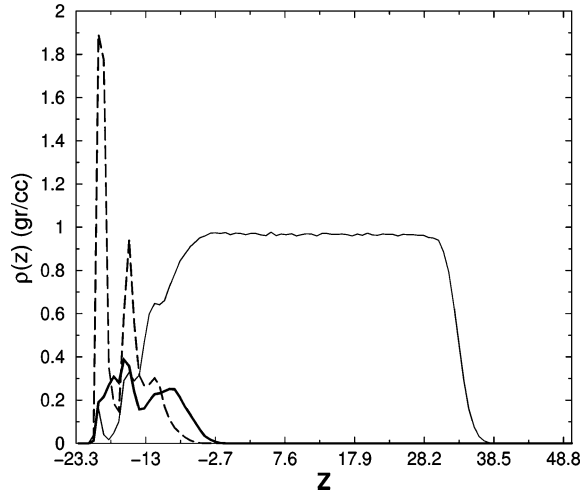


**Figure 2.** Density profiles for the SDS molecules on a graphite surface at low surface coverage. Water is depicted by the light solid line; the SDS head groups, by the dark solid line; and the SDS tails, by the dashed line. The graphite surface is located at the left of the plot.

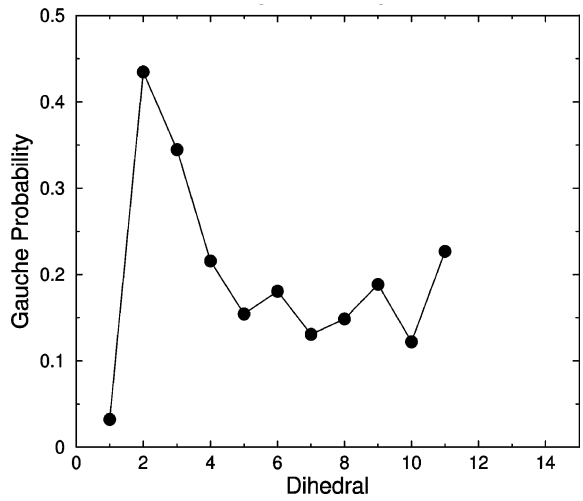


**Figure 3.** Probability of gauche defects as a function of carbon position of the surfactant molecules at low SDS surface coverage.

in all-trans conformation is $l \approx 15.0$ Å, the average length observed indicates that the tails were bent from their trans configuration, in agreement with the dihedral information given in Figure 3.

AFM experiments of the same system have been conducted to measure the height of the aggregate,[23] which is related to the radius of the hemicylinder, and an actual reference found for 2.8 mM SDS on graphite, a height of 17 Å.[23] In our case, we measured the average radius directly from the images (e.g., Figure 1) of the aggregate as the distance from the surface to the beginning of the tails (diameter in the *z*-direction), and we found an average radius of $l \approx 14$ Å. The diameter along the $X-Y$ plane (parallel to the interface) was about $l \approx 26$ Å. Those results suggested that the surfactant molecules aggregated in a hemicylindrical shape (Figure 1). If we add the headgroup diameter (≈3.0 Å) to the measured radius, we obtain a hemicylinder height of about $l = 17$ Å. However, a better estimation of the height can be obtained from the density profiles by measuring the distance from the first to the last points in the headgroup density profile. In this way, we found a height of $l = 17.3$ Å which is in good agreement to the value observed in the experiments. Even more, the length of the hemicilynder

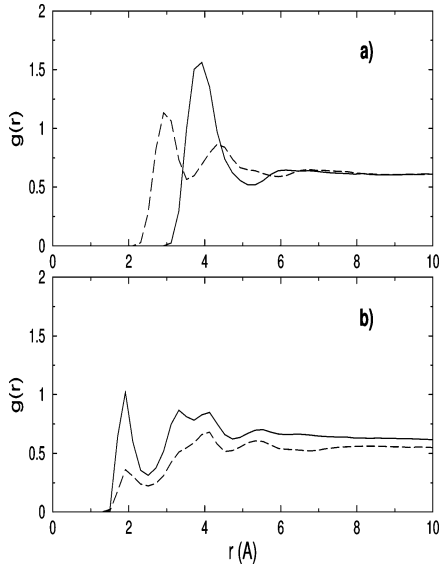


**Figure 4.** The radial distribution function of the head groups and water molecules at low SDS surface coverage: (a) $g_{S-OW}(r)$ (solid line) for S−OW groups (sulfur atom in SDS with water oxygens) and $g_{S-HW}(r)$ (dashed line) for S−HW groups (sulfur atom in SDS with water hydrogens), and (b) $g_{O_2-HW}(r)$ (solid line) for $O_2$-HW groups ($O_2$ oxygens in SDS with water hydrogens) and $g_{OS-HW}(r)$ (dashed line) for OS−HW groups (OS oxygen in SDS with water hydrogens).

is extended over one side of the solid plate (perpendicular view in Figure 1).

The study of the arrangement of water molecules around the surfactants was investigated by the pair correlation function ($g(r)$). In Figure 4a, the $g(r)$'s of the head groups with the water molecules are shown. It is observed that water oxygens are located at ≈4 Å from the sulfur atom (center of the head), defining the first solvation shell (see $g_{S-OW}(r)$ in Figure 4a). In addition, a second solvation shell can be observed at ≈6 Å from the sulfur atom. The $g(r)$ of the sulfur−water hydrogens ($g_{S-HW}(r)$) showed more structure, with two well-defined peaks, indicating that the most likely configuration of hydrogens is pointing to the headgroups, as suggested by the distance of these peaks compared with those of the $g_{S-OW}(r)$. Moreover, from the first solvation shell in $g_{S-HW}(r)$, we observed formation of hydrogen bonds between the oxygens of the head groups and the water hydrogens, as shown by the peaks in $g_{OS-HW}(r)$ and $g_{O_2-HW}(r)$ (Figure 4b). The second peak in $g_{O_2-HW}(r)$ (Figure 4b) splits in two, suggesting more structure of the water hydrogens in this vicinity, although the second peak in $g_{OS-HW}(r)$ did not show this feature clearly. However, in both pair correlation functions, $g_{O_2-HW}(r)$ and $g_{OS-HW}(r)$, a third peak was observed. In fact, all of these $g(r)$ structures suggest strong hydrogen bond interactions during the formation of the aggregates. It is worth mentioning that the system is inhomogeneous and nonsymmetric in the *z*-direction. Therefore, the $g(r)$'s of the surfactant−water do not go to unity as usual $g(r)$'s of bulk systems.

When the SDS surface coverage was increased on the surface, different features were observed. For instance, we obtained a picture of the aggregate that was different from that at low SDS surface coverage. From this system, we observed an evolution from a monolayer to a bilayer-like system for the first 1.8 ns (Figure 5a, b). Actually, at all times, the solid surface was covered with SDS molecules. Since the number of molecules for this simulation was double that at low concentration (which was already the number for the cmc for this surface), the solid area should have been already well coated by the surfactants.

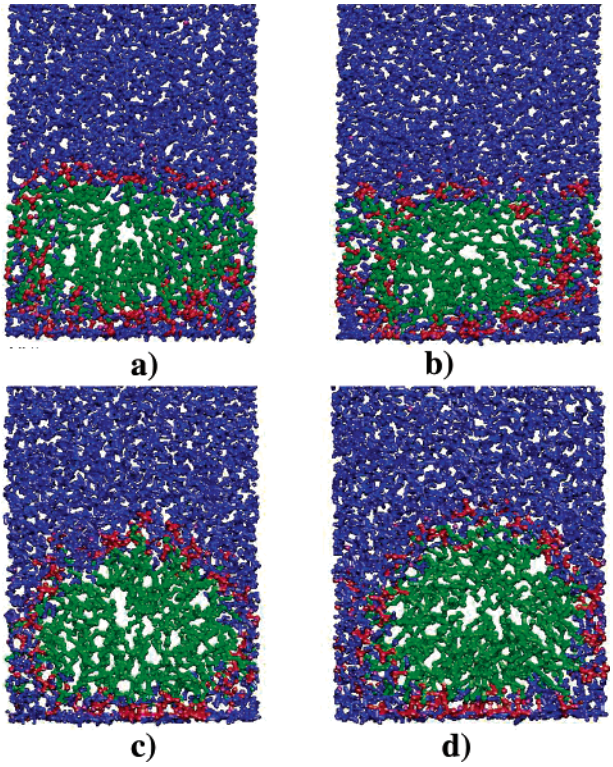


**Figure 5.** Snapshots of the SDS surfactant on the graphite surface at high SDS surface coverage for different simulation times: (a) 1.3 ns, (b) 1.8 ns, (c) 13.0 ns, and (d) 17.0 ns. Water is shown in blue; SDS headgroups, in red; SDS tails, in green; and the $Na^+$ counterions, in purple. The graphite plate is located at the bottom side of the molecules.

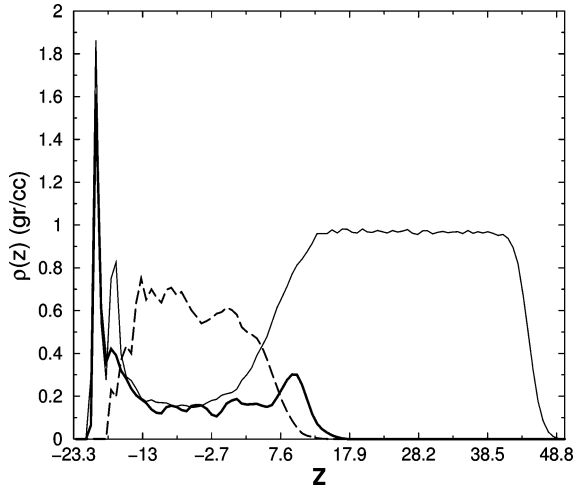


**Figure 6.** Density profiles for the SDS molecules on a graphite surface at high surface coverage. Water is depicted by the light solid line; the SDS head groups, by the dark solid line; and the SDS tails, by the dashed line. The graphite surface is located at the left of the plot.

In this case, the SDS headgroups arranged next to the solid surface, where some water molecules were also found. Moreover, those water molecules were absorbed at the solid surface, forming a well-defined layer (even a second layer can also be depicted) shown by the water density profile in Figure 6. Therefore, it seems that the attractive interactions between carbon tails and graphite atoms combined with the electrostatic repulsion among surfactant headgroups (which got close to the surface due to the absorbed water layer) exhibit a cylindrical aggregate-like form on the solid surface.

When we measured the total length of the tails, we found an average length of $l = 11.5$ Å, suggesting that the tails were straighter than those at low surface coverage. For completeness, we showed the probability of gauche defects for this system where we observed fewer oscillations at the end of the carbon tails, as compared with those at low surface coverage (Figure 7). The diameter of the aggregate (measured from the beginning of the tails in the pictures) in the *z*-direction and in the plane parallel to the interface ($X-Y$) were $l \approx 28$ Å and $l \approx 27$ Å, respectively. The measurement from the headgroup density profile was $l = 33.8$ Å, which is slightly smaller than the distance of two surfactant chains pointed tail-to-tail plus the headgroups ($l = 36$ Å). Moreover, the calculated radius on the *z*-axis for this system (16.9 Å) is slightly smaller than that calculated at low surface coverage. We also observed from Figure 6 that the hydrocarbon chains are away from the graphite surface, as compared with the water molecules. In fact, the tails are inside the headgroups core−shell, as indicated by the density profiles in Figure 6. Once again, these data suggested that the surfactant molecules assembled in a cylindrical shape (Figure 5d). As in the case at low surface coverage, the length of the

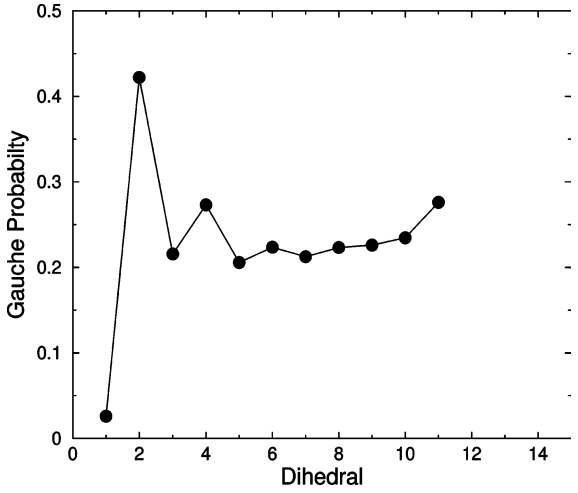


**Figure 7.** Probability of gauche defects as a function of carbon position of the surfactant molecules at high SDS surface coverage.

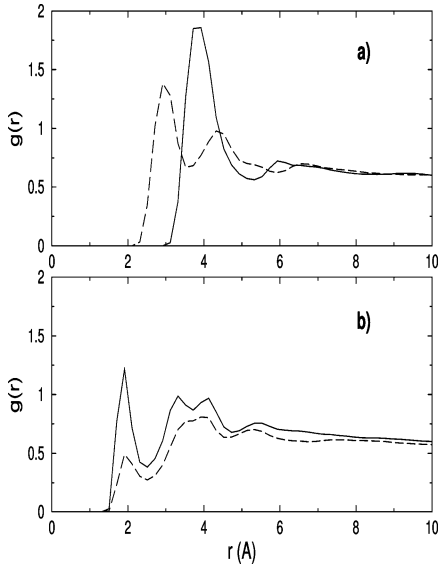


**Figure 8.** The radial distribution function of the head groups and water molecules at high SDS surface coverage. (a) $g_{S-OW}(r)$ (solid line) for S−OW groups (sulfur atom in SDS with water oxygens) and $g_{S-HW}(r)$ (dashed line) for S−HW groups (sulfur atom in SDS with water hydrogens). (b) $g_{O_2-HW}(r)$ (solid line) for $O_2$-HW groups ($O_2$ oxygens in SDS with water hydrogens) and $g_{OS-HW}(r)$ (dashed line) for OS−HW groups (OS oxygen in SDS with water hydrogens).

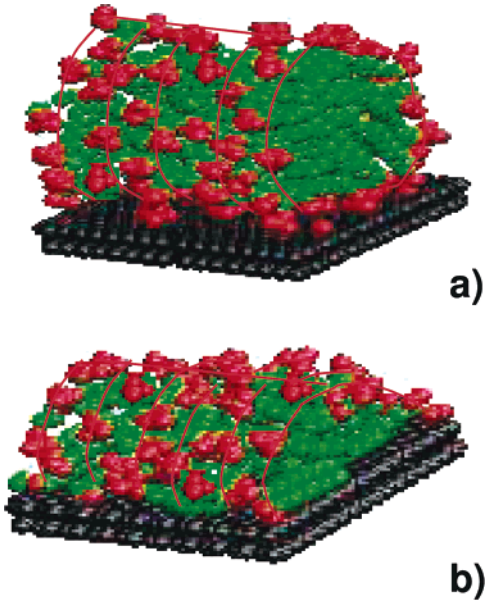


**Figure 9.** Snapshots, of the last configuration, of a lateral view of the SDS surfactant on the graphite surface at (a) high and (b) low surface coverage. The lines in the pictures are just to guide the form of the full-cylinder and the half-cylinder in parts a and b, respectively. For clarity, water molecules are not shown. The SDS headgroups are red, the SDS tails are green, and the graphite plate is black.

full cylinder is also extended all on one side of the graphite plate (Figure 9). Therefore, in both cases at low and at high SDS concentration, the aggregates seem to cover nearly all the surface area.

Finally, we also calculated the $g(r)$ of the water molecules around the SDS headgroups, and we found that peaks in the $g(r)$ (Figure 8) had shapes that are similar to those given at low SDS surface coverage. Therefore, these results suggested that the hydrogen bond formation is the same at both low and high concentrations.

## 4. Discussion and Conclusions

We performed a pair of computer experiments using molecular dynamics simulations for the SDS surfactant on a graphite surface. Two surface coverages were employed to study the formation of aggregates, and different features were observed in each case. At low concentration, the surfactant presents a hemicylindrical shape with the tail groups attached to the graphite surface. Moreover, from the simulations, we were able to observe how the tails of the surfactants were well adsorbed to the graphite plate, forming layers on the surface. The results agreed with experimental results observed in a similar system.

However, at high SDS surface coverage, the surfactants aggregate in a full cylinder with some headgroups next to the solid surface. Since graphite is a hydrophobic surface, this result seems to be opposite to that observed in the experiments.[23] As was mentioned before, there are surfactants that form different aggregates on different surfaces, for example, $C_{14}$TAB forms spherical micelles on amorphous silica and full cylinders on mica.[19] However, in the present work, we observed that the SDS forms not only half cylinders but also full cylinders on the same surface, graphite in this case.

The half cylinder aggregates at low surface coverage can be explained in terms of the affinity of the tail groups with the substrate through the van der Waals interactions. However, at high surface coverage, the van der Waals interactions seem to be not the primary interactions. Since the solid surface was well saturated (more than twice the surface coverage for this area) with surfactant molecules, the initial monolayer rapidly broke to form a bilayer-like system. Water molecules were adsorbed at the solid surface, forming a water layer (see Figure 5 and 6). By this way an "hydrophilic layer" (layer of water molecules) was created on the top of the graphite surface, then the self-assembly of the molecules continued until they had a stable structure, a full cylinder in this case. Moreover, since the full cylinder (as well as the half-cylinder) is extended along all the surface (Figure 9), the aggregate seems to be more stable, since there are several SDS headgroups attached to the water molecules that are well absorbed at the graphite plate. With this picture in mind, we reconcile the present results with those observed for the experiments; i.e., hydrophilic substrates form full cylinders. The interesting question here is how to make a hydrophobic surface hydrophilic in order to form full cylinders? A possibility would be by adding counterions on the surface, as stated in previous experiments of surfactants on gold substrates,[9] or by saturating the surface well above the surface coverage, as we did in the present work. In both cases, it was possible to form an "hydrophilic layer" on the actual substrate (the authors in ref 9 did not say it in these terms).

Finally, from these simulations, we showed more insights from the molecular point of view of the self-organization of surfactants on solid surfaces. The organization is determined by the substrate, which drives the interactions with the surfactant; however, the morphology of the surface might be altered by the surfactant concentration affecting the self-assembly of the molecules.

**Acknowledgment.** The author acknowledges support from CONACyT-Mexico through Grant 42842-F and from DGAPA-UNAM through Grant IN102207. Margarita Rivera is also thanked for helpful discussions of the manuscript.

### References and Notes

(1) Saccani, J.; Castano, S.; Beaurain, F.; Laguerre, M.; Desbat, B. *Langmuir* **2004**, *20*, 9190.
(2) Piasecki, D. A.; Wirth, M. J. *J. Phys. Chem.* **1993**, *97*, 7700.
(3) Tian, Y.; Umemura, J.; Takenaka, T. *Langmuir* **1988**, *4*, 1064.
(4) Higgins, D. A.; Naujok, R. R.; Corn, R. M. *Chem. Phys. Lett.* **1993**, *213*, 485.
(5) Conboy, J. C.; Messmer, M. C.; Richmond, G. *Langmuir* **1998**, *14*, 6722.
(6) Zhang, Z. H.; Tsuyumoto, I.; Kitamori, T.; Sawada, T. *J. Phys. Chem. B* **1998**, *102*, 10284.
(7) Lyttle, D. J.; Lu, J. R.; Su, T. J.; Thomas, R. K.; Penfold, J. *Langmuir* **1995**, *11*, 1001.
(8) Lu, J. R.; Hromadova, M.; Simister, E. A.; Thomas, R. K.; Penfold, J. *J. Phys. Chem.* **1994**, *98*, 11519.
(9) Jaschke, M.; Butt, H.-J.; Gaub, H. E.; Manne, S. *Langmuir* **1997**, *13*, 1381.
(10) Grant, L. M.; Tiberg, F.; Ducker, W. A. *J. Phys. Chem. B* **1998**, *102*, 4288.
(11) Ducker, W. A.; Wanless, E. J. *Langmuir* **1999**, *15*, 160.
(12) Ducker, W. A.; Grant, L. M. *J. Phys. Chem. B* **1996**, *100*, 11507.
(13) Manne, S.; Cleveland, J. P.; Gaub, H. E.; Stucky, G. D.; Hansma, P. K. *Langmuir* **1994**, *10*, 4409.
(14) McDermott, D. C.; McCarney, J.; Thomas, R. K.; Rennie, A. R. *J. Colloid Interface Sci.* **1994**, *162*, 304.
(15) Chandar, P.; Somasundaran, P.; Turro, N. J. *J. Colloid Interface Sci.* **1987**, *117*, 31.
(16) Pashley, R. M.; McGuiggan, P. M.; Horn, R. G.; Ninham, B. W. *J. Colloid Interface Sci.* **1988**, *126*, 569.
(17) Tilberg, F.; Jonsson, B.; Tang, J.; Lindmann, B. *Langmuir* **1994**, *10*, 2294.
(18) Levitz, P.; Van Damme, H. *J. Phys. Chem.* **1986**, *90*, 1302.
(19) Manne, S.; Gaub, H. E. *Science* **1995**, *270*, 1480.
(20) Patrick, H. N.; Warr, G. G.; Manne, S.; Aksay, I. A. *Langmuir* **1997**, *13*, 4349.
(21) Lau, C.; Furlong, D. N.; Healy, T. W.; Grieser, F. *Colloids Surf.* **1986**, *18*, 93.
(22) Binning, G; Quate, C. F.; Gerber, Ch. *Phys. Rev. Lett.* **1986**, *56*, 930.

(23) Wanless, E. J.; Ducker, W. A. *J. Phys. Chem.* **1996**, *100*, 3207.
(24) Yeo, Y. H.; Yackaboski, K.; McGonigal, G. C.; Thompson, D. J. *J. Vac. Sci. Technol.* **1992**, *A10*, 600.
(25) Krishnan, M.; Balasubramanian, S. *Phys. Chem. Chem. Phys.* **2005**, *7*, 2044.
(26) Bandyopadhyay, S.; Shelley, J. C.; Tarek, M.; Moore, P. B.; Klein, M. L. *J. Phys. Chem. B* **1998**, *102*, 6318.
(27) Werder, T.; Walther, J. H.; Jaffe, R. L.; Halicioglu, T.; Koumoutsakos, P. *J. Phys. Chem. B* **2003**, *107*, 1345.
(28) Srinivas, G.; Nielsen, S. O.; Moore, P. B.; Klein, M. L. *J. Am. Chem. Soc.* **2006**, *128*, 848.
(29) Kranenburg, M.; Venturoli, M.; Smit, B. *J. Phys. Chem. B* **2003**, *107*, 11491.
(30) Goetz, R.; Gompper, G.; Lipowsky, R. *Phys. Rev. Lett.* **1999**, *82*, 221.
(31) Shelley, J. C.; Shelley, M.; Reeder, R.; Bandyopadhyay, S.; Klein, M. L. *J. Phys. Chem. B* **2001**, *105*, 4464.
(32) Schweighofer, K. J.; Essmann, U.; Berkowitz, M. *J. Phys. Chem. B* **1997**, *101*, 3793.
(33) Dominguez, H.; Rivera, M. *Langmuir* **2005**, *21*, 7257.
(34) Forester, T. R.; Smith, W. DL-POLY Package of Molecular Simulation; CCLRC, Daresbury Laboratory: Daresbury, Warrington, England, 1996.
(35) Hoover, W. G. *Phys. Rev. A: At., Mol., Opt. Phys.* **1985**, *31*, 1695.
(36) Lu, J. R.; Marroco, A.; Su, T. J.; Thomas, R. K.; Penfold, J. *J. Colloid Interface Sci.* **1993**, *158*, 303.